Progress in Engineering Application and Technology Vol. 2 No. 1 (2021) 050-061


**PEAT**

Homepage: http://publisher.uthm.edu.my/periodicals/index.php/peat
e-ISSN : 2773-5303

# Fouling Mechanism of Ultrafiltration Polypiperazine Amide Membrane during Catalytic Conversion of Thiophene in Petroleum Fraction via Hybrid Membrane Photocatalytic Reactor (MPR)

**Faatihah Abdullah[1], Nur Hanis Hayati Hairom[1,2]***

[1]Department of Chemical Engineering Technology, Faculty of Engineering Technology,
Universiti Tun Hussein Onn Malaysia, 84600 Pagoh, Johor, MALAYSIA

[2]Microelectrics and Nanotechnology – Shamsudin Research Center, Institute for Integrated Engineering,
Universiti Tun Hussein Onn Malaysia, 86400, Parit Raja, MALAYSIA

*Corresponding Author Designation

DOI: https://doi.org/10.30880/peat.2021.02.01.005
Received 13 January 2021; Accepted 01 March 2021; Available online 25 June 2021

**Abstract**: In many centuries, petroleum industry has been established and greatly developed to produce many types of products such as gasoline, diesel, naphtha, kerosene and fuel oil. These products are obtained from the refinery and distillation of the crude oil. However, sulfur pollutants like thiophene subsequently contained in the petroleum products. Thiophene can cause deactivation of catalysts, promote formation of coke and damage the equipment including corrode the pipelines and pumping systems used in refining process. Membrane photocatalytic reactor (MPR) is the promising method that can degrade the sulfur pollutant in petroleum fraction. The zinc oxide-*Cymbopogon citratus* (ZnO-CC) nanoparticles was used due to its good photodegradation properties as well as the use of ultrafiltration polypiperazine amide (UF-PPA) membrane in this hybrid system. The drawback in utilization of the membrane is membrane fouling mechanisms that included complete blocking, intermediate blocking, standard blocking and cake formation may occurred during the photodegradation of thiophene and eventually affect the membrane flux decline. Therefore, this study aims to elucidate the correlation between flux decline and mechanism fouling of membrane via model fitting in MATLAB software. It was found that both stage1 and 2 shown that the occurrence of cake formation under pH 10, initial concentration of 50 ppm and ZnO-CC loading of 0.08 g/L. However, the cake formation may occur rapidly in first stage as the K value ($1.2\times10^{-3}$) is higher than K value ($7.8\times10^{-4}$) in second stage. As the result, the flux declines constantly leading to the highest value of flux decline (0.35). Whereas the lowest flux decline (0.09) was under solution pH 2, initial concentration of 100 ppm and photocatalyst

*Corresponding author: nhanis@uthm.edu.my

loading of 0.08. The initial concentration and photocatalyst loading also the parameters that can affect the thiophene degradation, but it is not critical as pH.

**Keywords**: Fouling Mechanism, Membrane, Catalytic Conversion, Thiophene, Petroleum Fraction, Blocking Filtration Law

## 1. Introduction

In Malaysia, the oil and gas industry has flourished and become the world's largest producers but this industry has been troubled with the present of pollutants. Most of the petroleum products and their feedstock including crude oil are polluted with sulfur compound that is thiophene. The sulfur occurred in integral part of petroleum coke matrix thus it is quite difficult to separate. Thiophene is aromatic heterocyclic compounds that contain stable conjugated rings and is made up of one sulfur as a heteroatom with chemical formula of $C_4H_4S$. Moreover, thiophene can cause the deactivation of catalysts, promote formation of coke and damage the equipment including corrode the pipelines and pumping systems used in refining process (Chen et al., 2020). In petroleum-based industries, thiophene can influence the manufacturing process and cause adverse harm to environment during petroleum refining and fuel combustion. Bian et al., 2019 had mentioned that sulphur dioxides and sulphur oxides gas would be released during the combustion of sulphur compound leading to occurrence of acid rain and land air pollution.

Hybrid membrane photocatalytic reactor (MPR) is a promising method which is the coupling system of photocatalytic degradation and membrane filtration for the effective thiophene degradation. The photocatalytic degradation will act as the pre-treatment process where it can reduce the membrane fouling and flux decline (Abu et al., 2020; Sidik, et al., 2019). Contrast to the conventional method that is sedimentation, coagulation and flocculation process, membrane filtration is used in this MPR system. The membrane can act as the barrier after the photocatalytic degradation process to filter some molecules or ions before discharging at the final stream. Additionally, the uses of MPR can give some benefits such as less energy consumption, better process control, has good efficiency and minimize the installation size. According to Ruby-figueroa et al., 2019, membrane technologies have received great interest over the conventional methodologies due to their advantages which are no uses of solvents and high efficiency of separation process. However, membrane fouling can be the critical issue that can affect the permeation flux. Also, the cleaning and replacement of membrane cause increase in the production costs and maintenance costs. Consequently, this will restrict or limit the uses of membrane despite its benefits of efficiency in filtration process. Thus, better understanding of the cause and mechanism of membrane fouling is important to minimise the problem.

In this study, the membrane fouling was determined via model fitting in MATLAB software and the correlation between the membrane flux decline and membrane fouling can be investigated through blocking filtration laws. In blocking filtration law, four different filtration mechanism which are complete blocking, standard blocking, intermediate blocking, and cake filtration that can be used to investigated the fouling phenomenon. Also, only a few studies that have used this software to analyse the membrane performance. Furthermore, it is a great challenge to identify and understand the fouling mechanism that occurred at a particular parameter like pH, initial concentration and photocatalyst loading. Moreover, the previous studies only investigate the fouling mechanism in industrial textile wastewater and palm oil mill secondary effluent (POMSE) treatment respectively. Therefore, this study had a significant outcome to the oil and gas industry including petroleum-based industries. This study could help the industries to control and optimize the parameters that can affect the fouling mechanism of the membrane.

1.1 Thiophene content in petroleum products

The sulfur content known as thiophene in crude oil is critically important to determine because the price of the crude oil is affected by sulfur. Crude oil can be classified into two types based on the amount of the sulfur. A “sweet” crude oil that has low sulfur content which is more preferable than “sour” crude oil that has high sulfur content. During crude oil refinery, sulfur can deactivate catalysts (Niyonsaba et al., 2018). Despite that, thiophene can generate benzene, hydrogen, methane, and hydrogen sulphide during the pyrolysis due to long heating time and high temperature. Figure 1 (a) shows the 3D structure of thiophene whereas Figure 1 (b) shows the Lewis structure of thiophene that show the presence of one sulphur atom and two double bonds. According to Wu et al., 2018, the presence of thiophene can be identified by the use of gas chromatography (GC) and also by high performance liquid chromatography (HPLC). When the thiophene came in contact with organisms, it can cause mutations and induce tumors (Zhang et al., 2020). Tang et al., 2020 had reported that the thiophene usually is difficult to remove due to its stable structure. Moreover, the thiophene’s C-S bonds need to be broken in order for effective removal of thiophene.

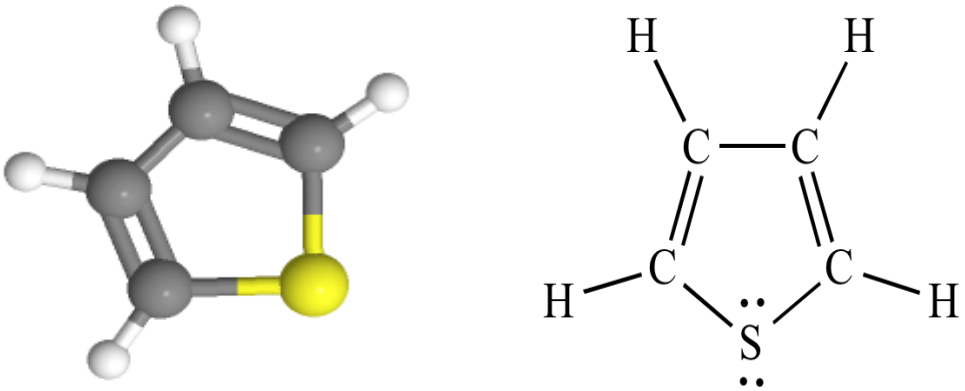


(a) (b)

**Figure 1: The thiophene diagram (a) 3-dimensional structure by ChemEssen.com (b) Lewis structure by chem.ucla.edu**

1.2 Membrane photocatalytic reactor (MPR)

Many studies regarding the potential of membrane photocatalytic reactor (MPR) compared with existing technologies. Despite the fact that photocatalytic degradation and membrane filtration process that associated in the MPR system will help in treatment of the thiophene content in the petroleum.

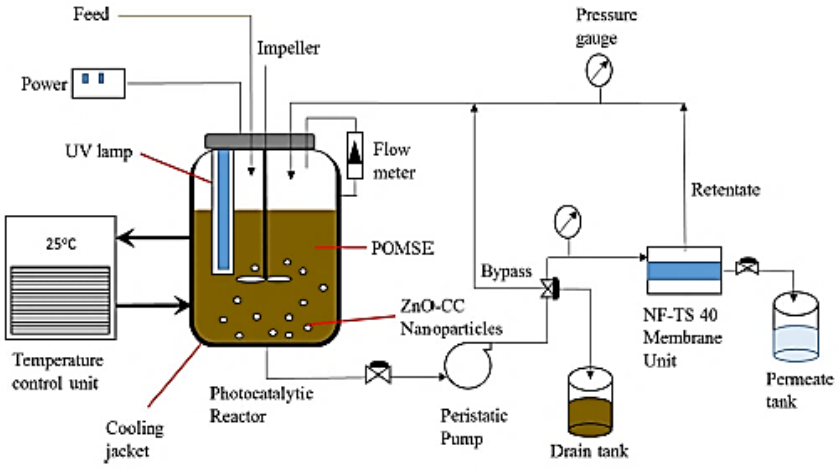


**Figure .2 :The schematic diagram of membrane photocatalytic reactor (MPR) [2]**

Figure 2 shows the illustration of thiophene treatment via MPR system. Recently, photocatalytic method shows high efficiency in degradation of thiophene. Generally, the photocatalyst undergo charge-transfer processes resulting in oxidation of thiophene once the light illumination energy is greater than the band gap (Khayyat & Roselin, 2016). With the help of the UV light in photocatalytic degradation of thiophene, the photocatalyst and the products can be separated simultaneously leading to reusability of the photocatalyst for another cycles (Sidik, et al., 2019). Some benefits of these hybrid system are the photocatalyst can be trapped in the reaction environment, simultaneous separation of photocatalyst and products during the continuous process and retention time of the molecules in the reactor can be controlled (Sidik, et al., 2019). In this study, zinc oxide-*Cymbopogon citratus* (ZnO-CC) nanoparticles and ultrafiltration polypiperazine amide (UF-PPA) membrane were used in the MPR system.

### 1.3 Zinc oxide-*Cymbopogon citratus* (ZnO-CC) photocatalyst

Currently, zinc oxide (ZnO) has been greatly used in many advanced technologies as the photocatalyst due to its several benefits. First and foremost, ZnO particles had the ability of UV absorption in a wide range of solar spectrum. Previously, Widiyandari et al., 2018 also reported that ZnO has gained attention because of its special property which is high photosensitivity that can stimulate the degradation of various pollutants that include thiophene. As well it can act as photocatalyst because its wide band gap. ZnO is an N-type semiconductor that has a wide band gap of 3.37 eV. Moreover, it has a large exciton binding energy which is 60 meV. These properties can lead to degradation of various pollutant including thiophene. In this study, ZnO-CC nanoparticles were used as its capability in photodegradation of the thiophene is very effective. This nanoparticle was synthesised via greener formulation that used plant-based such as *Cymbopogon citratus* leaf. It has potential as a reducing and capping agent that can inhibit the nanoparticles from overgrowth and agglomeration of particles can be reduced. Other than that, the size of ZnO-CC nanoparticles is smaller compared to commercial ZnO nanoparticles which have range of size ranging from 6.6–42.9 nm and 25–200 nm respectively. Thus, the agglomeration of ZnO-CC nanoparticles is less than commercial ZnO. Recently, Abu et al., 2020 had revealed that ZnO-CC showed higher photocatalytic degradation performance as well as its ability to reduce the membrane fouling compared to commercial ZnO.

### 1.4 Ultrafiltration polypiperazine amide (UF-PPA) membrane

A membrane is a semi-permeable layer that allows only selective components to pass through it and rejecting others unwanted component that will retain on the membrane surface or within the membrane and also can be considered as a permeable medium. In this study, the MPR system used ultrafiltration polypiperazine amide (UF-PPA) membrane and also known as “tight” UF membrane. Typically, the membrane with pore size or molecular weight cut-off (MWCO) of UF membranes ranging from 50 to 100 kDa that is used to recover the macromolecules such as suspended solids, proteins and carbohydrates whereas tight UF membranes from 1 to 3 kDa in which highly effective to concentrate low MWCO (Desa et al., 2019). For every different types of membranes, each membrane pores are characterised by their MWCO, where small MWCO will cause lower fluxes. Theoretically, the membrane has lower rejection of pollutants when the membrane pores are large and the MWCO are high. Meanwhile, the tendency of pollutant molecules to penetrate the membrane surface is high that can lead to the accumulation and compaction of the fouling cake layer. Then, this would affect permeate flow across the membrane during filtration. Thus, the membrane with lower MWCO can increase the permeate flux and leads to less severe membrane fouling. UF membrane had been utilized in industrial textile wastewater and the recovery of dye and minerals. This membrane has valuable retaining properties and exhibited fully dye degradation. Furthermore, Sun et al., 2020 had proved that ultrafiltration technology has been widely applied whether conventional or advanced method in treatment of drinking water.

## 2. Materials and Method

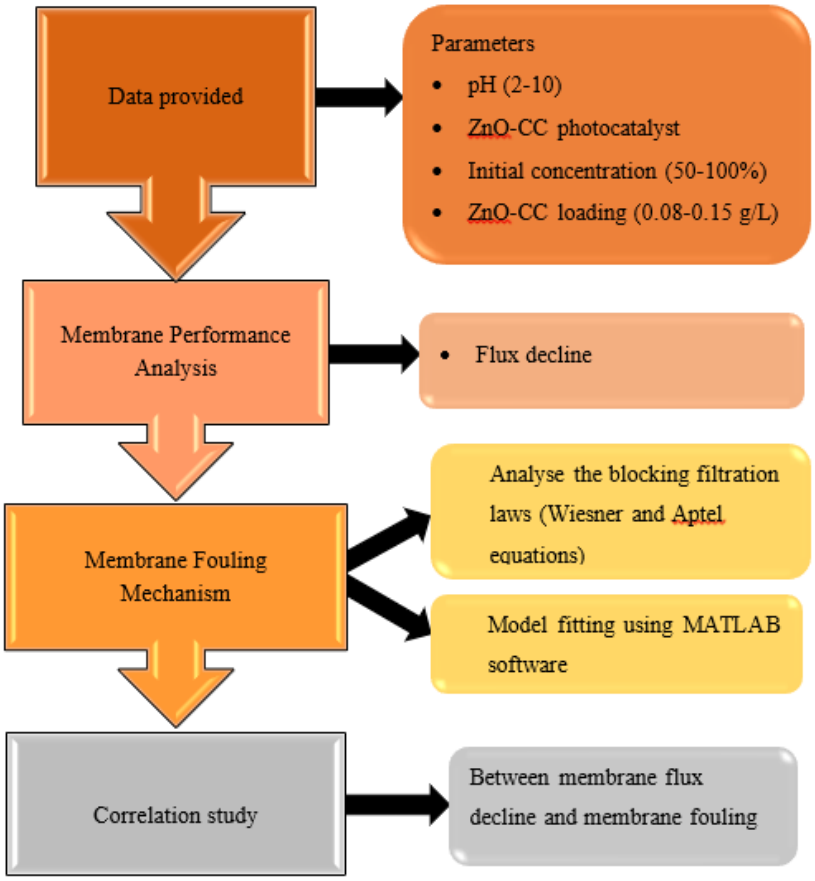


**Figure 2: Overview of research methodology**

2.1 Materials and apparatus

The materials and apparatus that have been used in this study are as follows:

• MATLAB software (MATLAB R2020a)
• Microsoft Excel (Excel 2013)

2.2 Methods

The analysis of membrane flux decline had been conducted under different pH, photocatalyst loading and initial concentration. Then, the graph of normalised flux decline during the filtration process of the petroleum through the membrane versus operating time were plotted in order to investigate the optimum condition for the operation of the membrane. The data provided was in normalised flux were converted to flux by using Eq. (2).

$$Normalised\ flux = \frac{Solution\ flux, J}{Free - thiophene\ petroleum, J_o} \qquad Eq.1$$

$$Then, \qquad flux = \frac{1}{normalised\ flux} = \frac{Free - thiophene\ petroleum, J_o}{Solution\ flux, J} \qquad Eq.2$$

The data provided in Microsoft Excel were imported to MATLAB software. From the linearized equation for each types of mechanism, the equations were simplified into $y = Kt + 1$ whereas y is varied according to the fouling mechanism. Then, the graphs were plotted via curve fitting in MATLAB software. The y-axis of the graph is the linearized equation for each mechanism while the x-axis of the

graph is the operating time. According to Sidik et al., 2019, degree of model fitness ($R^2$) and coefficient (K) were obtained from the graph and they are used as indicators in order to elucidate the fouling mechanism of the membrane. After that, the fouling mechanism of membrane was evaluated according to the theory of block filtration laws. From Figure 3, this law comprised (a) complete blocking, (b) standard blocking, (c) intermediate blocking, and (d) cake formation (Sidik et al., 2019). For each of the condition with different parameter value, two stages of blocking mechanism were identified and presented by two different slopes.

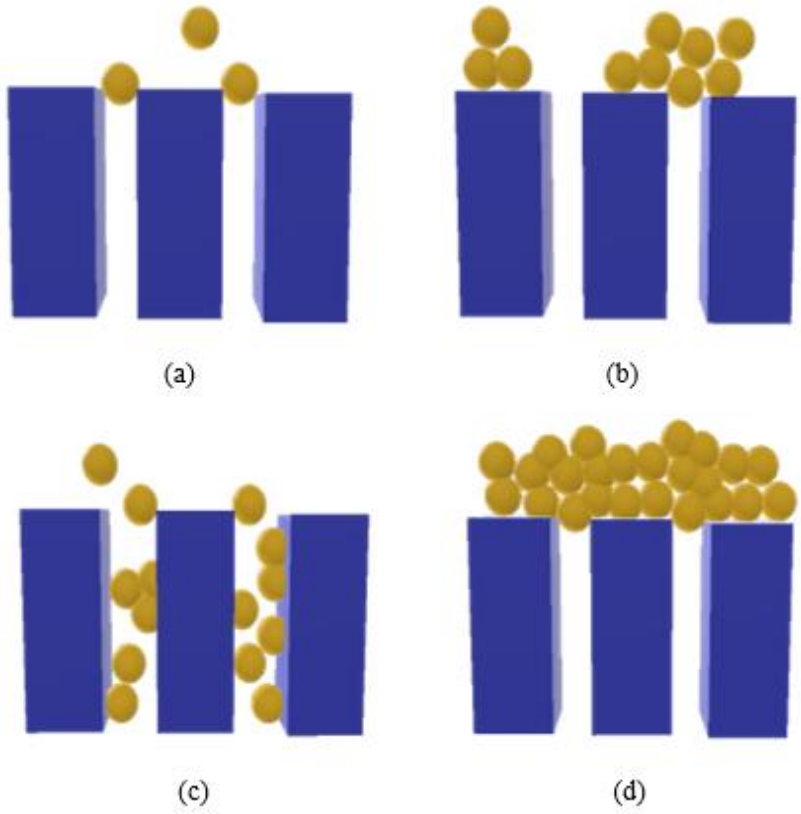


**Figure 3: The schematic drawing of membrane fouling mechanism (a) complete blocking (b) intermediate blocking (c) standard blocking (d) cake formation**

2.5 Blocking filtration laws

The blocking filtration laws were applied in scrutinizing the membrane fouling phenomenon. This law were established by Hermia et al. 1982 and systemized by Wiesner and Aptel in 1996 that present two stages of blocking mechanism with two different slopes (Desa et al., 2019). The constant membrane resistant, constant pressure drop and a specific resistance of the cake that is consistent with time are the assumptions in modifying the model. This model includes four different mechanisms which are complete blocking, standard blocking, intermediate blocking and cake formation with the linearized equation for each of the mechanism. For both complete blocking and intermediate blocking described that the plugging of the pores is caused by particles that reach the membrane surface (Iritani & Katagiri, 2016). Then, the membrane pores were blocked by the particles. However, there is slightly dissimilarity between these two mechanisms which is the particles do not overlap in complete blocking. In contrast with the intermediate blocking, there is overlapping of the particles or forming multi-layers on the membrane surface (Sidik et al., 2019). Iritani & Katagiri, 2016 reported that the applicable of these two mechanisms when the pore size is smaller than the diameter of the particle. Thus, the particle will trap on the surface of the membrane. As for the standard blocking, the pore is being constricting with the deposition of the particles onto the wall of the pore. Recently, Sidik et al., 2019 had assumed that volume of the membrane pore depends on the volume of the permeate proportionally. The formation of

the cake on the membrane surface is initiated by the pore blocking by particles and at the same time, more number particles deposited onto the other particles. An assumption for cake formation which is the cake resistance is proportional to the volume of cumulative filtered. As shown in Table 1, constant n that are influenced by the fouling mechanism whereas coefficient, K that are acquired from the slopes of the linear curves.

**Table 1: The blocking filtration laws with linearized equation [5]**

| Blocking Filtration Laws | n | Linearized Equation |
|---|---|---|
| Complete blocking model | 2 | $-ln\left(\frac{J_0}{J}\right) - 1 = Kt$ |
| Intermediate blocking model | 1 | $\frac{J_0}{J} - 1 = Kt$ |
| Standard blocking model | 1.5 | $\sqrt{\frac{J_0}{J}} - 1 = Kt$ |
| Cake formation model | 0 | $\left(\frac{J_0}{J}\right)^2 - 1 = Kt$ |

## 3. Results and Discussion

### 3.1 Analysis of flux decline

The analysis of membrane flux decline had been conducted under different pH, photocatalyst loading and initial concentration. These parameters were analysed via plotting graph of normalised flux for easy comparison vs. operating time in hour.

#### 3.1.1 MPR Run 1 under ph10, initial concentration of 50 ppm and 0.08 g/L photocatalyst loading

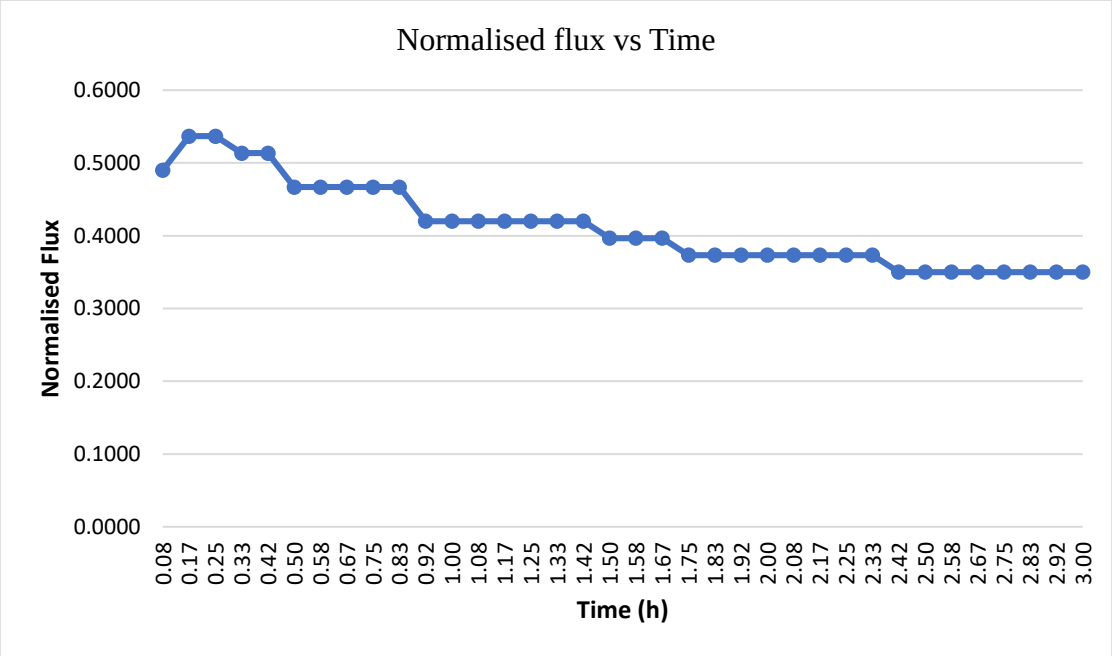


**Figure 4: Graph of normalised flux vs. time under pH10, initial concentration of 50ppm and ZnO-CC loading of 0.08 g/L**

Based on the Figure 5, the normalised flux was fluctuated for the first 0.42 hours. At 0.52 hours, it starts to decrease and constant until 0.83 hours with normalised flux approximately 0.46. For the next hours until 1.42 hour, it decreases and became constant again with approximately 0.42 of normalised

flux value. As the operating time reach 1.50 hours, the normalised flux slightly decreases and constant at approximately 0.40 for a short time until 1.67 hour. After that, it continues to decrease with constant value of 0.37 for a longer time until 2.33 hours. Lastly, the normalised flux stop declines at value of 0.35 and remain constant until the last hour.

3.1.2 MPR Run 20 under ph2, initial concentration of 100 ppm and 0.08 g/L photocatalyst loading

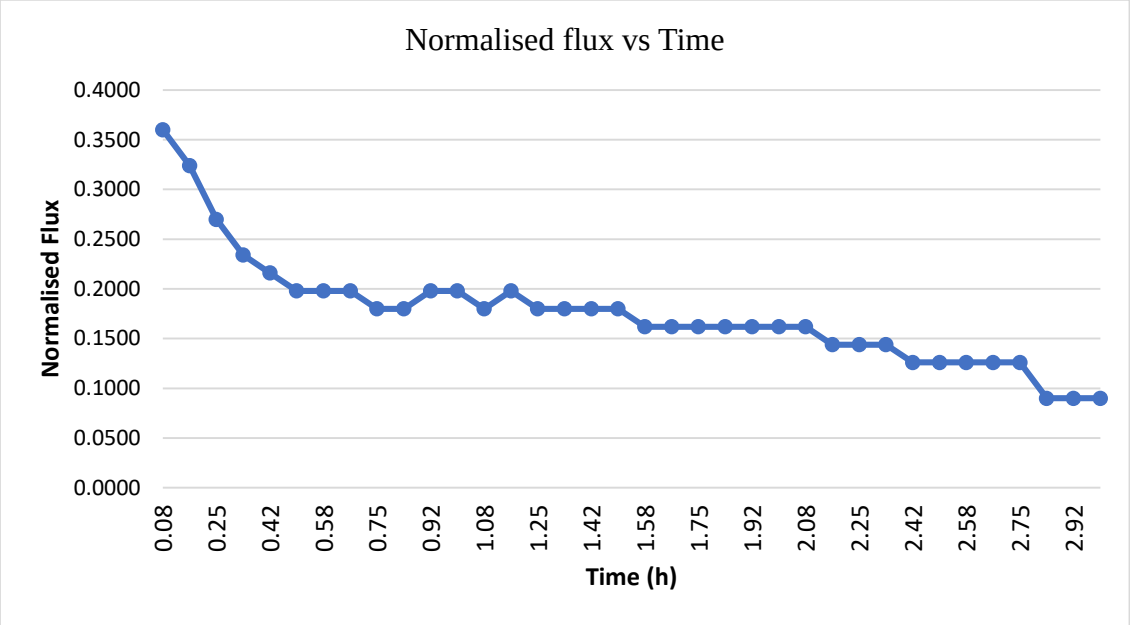


**Figure 5: Graph of normalised flux vs. time under pH 2, initial concentration of 100ppm and ZnO-CC loading of 0.08 g/L**

Based on the Figure 5 that show the relationship between normalised flux vs. time under ph 2, initial concentration of 100ppm and ZnO-CC loading of 0.08 g/L. For the first 0.42 hour, the normalised flux gradually decreases until its value reach 0.23. At 0.50 hours, it starts to remain constant only for a while until 0.67 hours with normalised flux of 0.20 and the fluctuation occurred until 1.17 hour. For the next hours until 1.50 hour, it slightly decreases 0.18 and remain constant. Then, the normalised flux slightly decreases again to 0.16 and remain constant at the longest time until 2.08 hour. As the operating time reach 2.17 hours, the normalised flux slightly decreases and constant at approximately 0.14 until 2.33 hour. At 2.42 hour until 2.75 hour, it decreases and remain constant at 0.12. Lastly, the normalised flux stop declines at value of 0.09 and remain constant until the last hour.

3.2 Analysis of membrane fouling mechanism

The mechanism of the membrane fouling was investigated by theory of block filtration laws via curve fitting in MATLAB software. In the model, the linearized equation for each of the blocking mechanism and the parameters data were fitted resulting in plotting a graph of linearized equation against time. The y-axis of the graph that were plotted represent the mechanisms meanwhile x-axis represent operating time. From the graph, $R^2$ and K were obtained which represent the model fitness degree and coefficient respectively (Sidik et al., 2019). Next, the degree of model fitness ($R^2$) and fitted parameter coefficient (K) were tabulated to determine the fouling mechanism that occurred for that parameters. Then, membrane fouling mechanism can be elucidated by referring to the $R^2$ and K as the indicators.

3.2.1 MPR Run 1 under ph10, initial concentration of 50 ppm and 0.08 g/L photocatalyst loading

**Table 2: The value of $R^2$ and K for pH10, initial concentration of 50 ppm and ZnO-CC loading of 0.08 g/L**

| Blocking mechanism | Stage 1 | | Stage 2 | |
|---|---|---|---|---|
| | $R^2$ | K | $R^2$ | K |
| Complete | -4.51 | $-5.494\times10^{-4}$ | -1.21 | $-2.410\times10^{-4}$ |
| Intermediate | 0.58 | $3.820\times10^{-4}$ | 0.78 | $2.089\times10^{-4}$ |
| Standard | 0.29 | $1.523\times10^{-4}$ | 0.55 | $7.863\times10^{-5}$ |
| Cake formation | 0.76 | $1.253\times10^{-3}$ | 0.91 | $7.834\times10^{-4}$ |

Based on the Table 2, the data obtained were divided into two stages in between the 4800 seconds. According to Table 2 the cake formation mechanism may occur during stage 1 as the value of $R^2$ is the highest compared to the other three mechanisms. This may be caused by the accumulation of particles on the surface of the membrane. However, it might not be too severe as the value of $R^2$ not exceed more than 0.90. As for the stage 2, the occurrence of cake formation is more significant as the value of $R^2$ is the highest which is 0.91. This is due to large number of particles that had accumulated on the membrane surface and had blocked the membrane pores.

3.2.2 MPR Run 20 under ph2, initial concentration of 100 ppm and 0.08 g/L photocatalyst loading

**Table 3: The value of $R^2$ and K for ph2, initial concentration of 100 ppm and ZnO-CC loading of 0.08 g/L**

| Blocking mechanism | Stage 1 | | Stage 2 | |
|---|---|---|---|---|
| | $R^2$ | K | $R^2$ | K |
| Complete | -0.90 | $-7.991\times10^{-4}$ | -0.19 | $-3.628\times10^{-4}$ |
| Intermediate | 0.76 | $1.264\times10^{-4}$ | 0.93 | $8.100\times10^{-4}$ |
| Standard | 0.57 | $3.851\times10^{-4}$ | 0.82 | $2.119\times10^{-5}$ |
| Cake formation | 0.83 | $7.879\times10^{-3}$ | 0.74 | $7.489\times10^{-3}$ |

Based on the Table 3, the data obtained were divided into two stages in between the 4800 seconds. Based on the result in Table 3, the cake formation mechanism may occur during stage 1 as the value of $R^2$ is the highest compared to the other three mechanisms which is 0.83. This phenomenon probably occurred due to the accumulation of particles on the surface of the membrane. Leading to the blockage of the membrane pores. As for the stage 2, the intermediate blocking mechanism is more significant to occur as the value of $R^2$ the highest which is 0.93. Although cake formation mechanism occurs in stage 1 but it only an assumption that it had possibility to occur. Thus, this implicate that the particles are in the formed of multilayer on the surface of the membrane that had blocked the membrane pores.

3.3 Correlation between flux decline and fouling mechanism

According to the both tables, the $R^2$ values for complete blocking mechanism were negative value which means it was very poor and is insignificant in the ultrafiltration of the solution. Probably, due to the various solute sizes which may not allow every solute to participate in blocking the entrance of the membrane pores completely. As for pH 2 with initial concentration of 100 ppm and ZnO-CC loading of 0.08 g/L, the possibility of cake formation to occur is low in the first stage but intermediate blocking mechanism had occurred during second stage. However, cake formation may rapidly occur that caused gradually membrane flux decline as the value of K ($7.9\times10^{-3}$) at initial filtration is higher than in the second filtration which is $8.1\times10^{-4}$. Moreover, the flux decline for this condition is the lowest that is 0.09 as the initial concentration is high whereas the ZnO-CC loading is low. Thus, this means that the amount of the photocatalyst is not sufficient to degrade the thiophene molecules. Leading to low efficiency in degradation of the thiophene and small volume of free thiophene petroleum were obtained. Next, solution pH of 10 that can be considered as alkaline solution. For the pH 10 with initial

concentration of 50 ppm and ZnO-CC loading of 0.08 g/L, both stages shown that the occurrence of cake formation. However, the possibility for cake formation to occur in first stage is lower than in second stage. Subsequently, rapid cake formation occur in first stage as the value of K ($1.2\times10^{-3}$) is higher than value of K ($7.8\times10^{-4}$) in second stage. As the result from the rapid cake formation, the flux declines constantly until the last hour and its value is the highest which is 0.35. This result related to the both low initial concentration and ZnO-CC loading. Although the photocatalyst loading is low that indicate small number of photocatalyst particles but it is sufficient to degrade the thiophene. As a result, large volume of free-thiophene petroleum were obtained.

For both stages, mostly cake formation mechanism had occurred and only a few times that the intermediate blocking mechanism would occur. Based on the data analysis, it was found that the flux decline of solution with pH 10 (0.35, 0.26, 0,20, 0.23) regarding the four different conditions is higher than flux decline with solution pH 2 (0.18, 0.17, 0.15, 0.09). It can be concluded that under alkaline conditions there was low reduction in flux occurred while under acidic conditions, the reduction in flux was high. Besides that, the flux decline is the higher when the ZnO-CC loading is higher as the photodegradation rate increases. This is resulting from the increasing in number of reaction sites on the photocatalyst surface that can help in adsorption of UV light. Eventually increase in number of hydroxyl radicals that responsible for the degradation of the pollutants. This can be observed under the ZnO-CC loading of 0.08 g/L was compared with 0.15 g/L with the same conditions that are pH 2 and initial concentration of 100 ppm. The latter condition produced high flux decline which means large volume of free-thiophene petroleum were obtained. Then, the initial concentration can affect the photodegradation rate of thiophene because as the initial concentration increase, the number of the photocatalyst needed also increase. For the initial concentration 50 ppm with pH 10 and ZnO-CC loading of 0.08 g/L, the flux decline is the highest which is 0.35. However, with the same condition but different initial concentration of 100 ppm, the flux decline is lower which is 0.20. As we can observed that, the higher initial concentration of solution, the lower the flux decline. Therefore, high demand of photocatalyst is needed in degradation of thiophene when the concentration is high. Additionally, this means that the production of free-thiophene petroleum also getting lower. This situation also related to hydroxyl radicals' generation that would be insufficient because the amount of hydroxyl ions produced is not correspond to the concentration of pollutant molecules.

## 4. Conclusion

Primarily, the flux decline that are proportionally related to the volume of free-thiophene petroleum produced and the four different fouling mechanisms (complete blocking, intermediate blocking, standard blocking and cake formation) including the correlation between the flux decline and fouling mechanism were studied. From the data analysis, both stages shown that the occurrence of cake formation under pH 10 with initial concentration of 50 ppm and ZnO-CC loading of 0.08 g/L. However, the cake formation may occur rapidly in first stage as the K value ($1.2\times10^{-3}$) is higher than K value ($7.8\times10^{-4}$) in second stage. As the result from the rapid cake formation, the flux declines are constant until the last hour leading to the highest value of flux decline which is 0.35. As for pH 2 with initial concentration of 100 ppm and ZnO-CC loading of 0.08 g/L, cake formation may rapidly occur in the initial filtration that caused gradually membrane flux decline as the K value ($7.9\times10^{-3}$) is higher than K value ($8.1\times10^{-4}$) in the second filtration. However, intermediate blocking mechanism occurs during second filtration. Based on all conditions, the cake formation mostly occurred for both stages. Besides, it clearly shown that under solution pH 10, initial concentration of 50 ppm and photocatalyst loading of 0.08 g/L have the highest flux decline (0.35) whereas the lowest flux decline was under solution pH 2, initial concentration of 100 ppm and photocatalyst loading of 0.08 g/L when comparing with the other conditions. It was also found that the flux decline of solution with pH 10 (0.35, 0.26, 0,20, 0.23) regarding the four different conditions is higher than flux decline with solution pH 2 (0.18, 0.17, 0.15, 0.09). It can be concluded that low reduction of flux happened under alkaline conditions, meanwhile the reduction of flux was high under acidic conditions. These results showed that pH solution was the

critical parameter that need to be highly considered in degrading the thiophene. The initial concentration and photocatalyst loading also the parameters that can affect the thiophene degradation, but it is not critical as pH. These two parameters were related to each other as the photocatalyst loading is low which indicates small number of photocatalyst particles were used while the initial concentration is high. Thus, the amount of the photocatalyst might not be sufficient to degrade the thiophene molecules that lead to low efficiency in degradation of the thiophene. Therefore, small volume of free thiophene petroleum were obtained.

**Acknowledgement**

The authors would like to thank the Faculty of Engineering Technology, Universiti Tun Hussein Onn Malaysia for its support.

**References**

[1] Abu, D., Sidik, B., Hanis, N., & Hairom, H. (2020). Performance of membrane photocatalytic reactor incorporated with ZnO-Cymbopogon citratus in treating palm oil mill secondary effluent. *Process Safety and Environmental Protection*, *143*, 273–284. https://doi.org/10.1016/j.psep.2020.06.038

[2] Abu, D., Sidik, B., Hanis, N., Hairom, H., Wahab, A., & Abdul, N. (2020). Chemical Engineering Research and Design The potential control strategies of membrane fouling and performance in membrane photocatalytic reactor ( MPR ) for treating palm oil mill secondary effluent ( POMSE ). *Chemical Engineering Research and Design*, *162*, 12–27. https://doi.org/10.1016/j.cherd.2020.07.021

[3] Bian, H., Zhang, H., Li, D., Duan, Z., Zhang, H., & Zhang, S. (2019). Microporous and Mesoporous Materials Insight into the oxidative desulfurization mechanism of aromatic sulfur compounds over Ti-MWW zeolite : A computational study. *Microporous and Mesoporous Materials*, *August*, 109837. https://doi.org/10.1016/j.micromeso.2019.109837

[4] Chen, X., Li, H., Zhang, L., Shi, Q., Zhao, S., & Xu, C. (2020). Direct sulfur-containing compounds analysis in petroleum via (+) ESI FT-ICR MS using HBF4 as ionization promoter. *Fuel*, *278*(December 2019), 118334. https://doi.org/10.1016/j.fuel.2020.118334

[5] Desa, A. L., Hairom, N. H. H., Ng, L. Y., Ng, C. Y., Ahmad, M. K., & Mohammad, A. W. (2019). Industrial textile wastewater treatment via membrane photocatalytic reactor (MPR) in the presence of ZnO-PEG nanoparticles and tight ultrafiltration. *Journal of Water Process Engineering*, *31*(January), 100872. https://doi.org/10.1016/j.jwpe.2019.100872

[6] Desa, A. L., Hairom, N. H. H., Sidik, D. A. B., Misdan, N., Yusof, N., Ahmad, M. K., & Mohammad, A. W. (2019). A comparative study of ZnO-PVP and ZnO-PEG nanoparticles activity in membrane photocatalytic reactor (MPR) for industrial dye wastewater treatment under different membranes. *Journal of Environmental Chemical Engineering*, *7*(3), 103143. https://doi.org/10.1016/j.jece.2019.103143

[7] Hairom, N. H. H., Mohammad, A. W., & Kadhum, A. A. H. (2014). Nanofiltration of hazardous Congo red dye: Performance and flux decline analysis. *Journal of Water Process Engineering*, *4*(C), 99–106. https://doi.org/10.1016/j.jwpe.2014.09.008

[8] Iritani, E., & Katagiri, N. (2016). Developments of blocking filtration model in membrane filtration. *KONA Powder and Particle Journal*, *2016*(33), 179–202. https://doi.org/10.14356/kona.2016024

[9] Khayyat, S., & Roselin, L. S. (2016). Photocatalytic degradation of Benzothiophene and Dibenzothiophene using Supported Gold Nanoparticle Abstract : Photocatalytic oxidation of

benzothiophene ( BT ) and dibenzothiophene ( DBT ). *Journal of Saudi Chemical Society*. https://doi.org/10.1016/j.jscs.2016.11.001

[10] Niyonsaba, E., Manheim, J. M., Yerabolu, R., & Kenttamaa, H. I. (2018). *Recent Advances in Petroleum Analysis by Mass Spectrometry Recent Advances in Petroleum Analysis by Mass Spectrometry*. https://doi.org/10.1021/acs.analchem.8b05258

[11] Ruby-figueroa, R., Nardi, M., Sindona, G., Conidi, C., & Cassano, A. (2019). *A Multivariate Statistical Analyses of Membrane Performance in the Clarification of Citrus Press Liquor*. https://doi.org/10.3390/chemengineering3010010

[12] Sidik, D. A. B., Hairom, N. H. H., & Mohammad, A. W. (2019). Performance and fouling assessment of different membrane types in a hybrid photocatalytic membrane reactor (PMR) for palm oil mill secondary effluent (POMSE) treatment. *Process Safety and Environmental Protection*, *130*, 265–274. https://doi.org/10.1016/j.psep.2019.08.018

[13] Sun, F., Xu, Y., Li, M., Zhang, Y., Wang, Y., Zhang, Y., & Zhang, D. (2020). Journal of Water Process Engineering Membrane cleaning of ultrafiltration in the combined membrane filtration processes and health risk assessment. *Journal of Water Process Engineering*, *38*(May), 101584. https://doi.org/10.1016/j.jwpe.2020.101584

[14] Tang, L., Long, K., Chen, S., Gui, D., & He, C. (2020). Removal of thiophene sulfur model compound for coal by microwave with peroxyacetic acid. *Fuel*, *272*(April), 117748. https://doi.org/10.1016/j.fuel.2020.117748

[15] Widiyandari, H., Ketut Umiati, N. A., & Dwi Herdianti, R. (2018). Synthesis and photocatalytic property of Zinc Oxide (ZnO) fine particle using flame spray pyrolysis method. *Journal of Physics: Conference Series*, *1025*(1). https://doi.org/10.1088/1742-6596/1025/1/012004

[16] Wu, W. B., Xue, S., Chen, J. H., & Li, X. (2018). High removal of thiophene from model gasoline by porous MIL-101(Cr)/SA hybrid membrane. *RSC Advances*, *8*(71), 41003–41011. https://doi.org/10.1039/C8RA06579A

[17] Zhang, X. C., Wu, S. H., Jia, S. Y., Wang, C., Sun, S. W., Wang, X. M., Meng, Z. H., Lin, Y. Y., Liu, Y., Ren, H. T., & Han, X. (2020). Turning thiophene contaminant into polymers from wastewater by persulfate and CuO. In *Chemical Engineering Journal* (Vol. 397). Elsevier B.V. https://doi.org/10.1016/j.cej.2020.125351